LmrR-mediated gene regulation of multidrug resistance in Lactococcus lactis

Agustiandari, Herfita; Peeters, Eveline; de Wit, Janny G.; Charlier, Daniel; Driessen, Arnold J. M.

Published in:
Microbiology-Sgm

DOI:
10.1099/mic.0.048025-0

Publication date:
2011

Microbiology (2011), **157**, 1519–1530 **DOI** 10.1099/mic.0.048025-0

LmrR-mediated gene regulation of multidrug resistance in *Lactococcus lactis*

Herfita Agustiandari,[1] Eveline Peeters,[2] Janny G. de Wit,[1] Daniel Charlier[2] and Arnold J. M. Driessen[1]

Correspondence
Arnold J. M. Driessen
a.j.m.driessen@rug.nl

[1]Department of Microbiology, Groningen Biomolecular Sciences and Biotechnology Institute and The Kluyver Centre for the Genomics of Industrial Fermentation, University of Groningen, Nijenborgh 7, 9747 AG Groningen, The Netherlands

[2]Erfelijkheidsleer en Microbiologie, Vrije Universiteit Brussel (VUB), Pleinlaan 2, B-1050 Brussels, Belgium

Received 6 January 2011
Revised 13 February 2011
Accepted 14 February 2011

Multidrug resistance (MDR) in *Lactococcus lactis* is due to the expression of the membrane ATP-binding cassette (ABC) transporter LmrCD. In the absence of drugs, the transcriptional regulator LmrR prevents expression of the *lmrCD* operon by binding to its operator site. Through an autoregulatory mechanism LmrR also suppresses its own expression. Although the *lmrR* and *lmrCD* genes have their own promoters, primer extension analysis showed the presence of a long transcript spanning the entire *lmrR–lmrCD* cluster, in addition to various shorter transcripts harbouring the *lmrCD* genes only. 'In-gel' Cu-phenanthroline footprinting analysis indicated an extensive interaction between LmrR and the *lmrR* promoter/operator region. Atomic force microscopy imaging of the binding of LmrR to the control region of *lmrR* DNA showed severe deformations indicative of DNA wrapping and looping, while LmrR binding to a fragment containing the *lmrCD* control region induced DNA bending. The results further suggest a drug-dependent regulation mechanism in which the *lmrCD* genes are co-transcribed with *lmrR* as a polycistronic messenger. This leads to an LmrR-mediated regulation of *lmrCD* expression that is exerted from two different locations and by distinct regulatory mechanisms.

INTRODUCTION

In their natural environment, bacteria have to cope with naturally occurring toxic molecules (plant alkaloids, bile salts), harmful metabolic end-products, antimicrobial peptides, and secondary metabolites such as antibiotics. A widespread mechanism to counteract the inhibitory action of such molecules is their secretion from the cell by membrane-bound multidrug resistance (MDR) transporters (Chopra & Roberts, 2001; Neyfakh *et al.*, 1991; Tennent *et al.*, 1985). For instance, the cationic berberine alkaloids produced by many plants are substrates for MDR pumps, such as QacA and NorA of *Staphylococcus aureus* (Hsieh *et al.*, 1998; Neyfakh *et al.*, 1993; Ng *et al.*, 1994; Schumacher & Brennan, 2003). Soil- or plant-associated organisms display the highest abundance of chromosomally encoded MDR efflux systems (Paulsen *et al.*, 2000; Saier *et al.*, 1998). MDR transporters are often subject to regulatory control (Grkovic *et al.*, 2002), as their expression at a high level may be critical to cells (Eckert & Beck, 1989; Gury *et al.*, 2004). The expression of most MDR transporters is either positively or negatively controlled by local regulatory proteins (Eckert & Beck, 1989; Hickman *et al.*, 1990) and/or globally by stress-related regulators. For example, the overexpression of the *acrAB* MDR locus in *Escherichia coli* is regulated by the global regulators MarA, Rob and SoxS, the local repressor AcrR (Alekshun & Levy, 1997; Ma *et al.*, 1996), and the quorum sensor regulator SdiA (Rahmati *et al.*, 2002).

The Gram-positive bacterium *Lactococcus lactis* plays a major role in fermented dairy food production. *L. lactis* readily develops an MDR phenotype upon long-term exposure to structurally unrelated compounds such as daunomycin, Hoechst 33342, ethidium bromide, rhodamine 6G and cholate (Bolhuis *et al.*, 1994; Lubelski *et al.*, 2004; Mazurkiewicz *et al.*, 2004). This MDR phenotype is due to the constitutive expression of the *lmrCD* genes, which encode a heterodimeric ATP-binding cassette (ABC) MDR transporter that secretes these compounds from the cell (Lubelski *et al.*, 2006). Expression of the *lmrCD* genes is controlled by a local transcriptional regulator termed LmrR (Agustiandari *et al.*, 2008). LmrR acts as a drug-sensitive

Abbreviations: ABC, ATP-binding cassette; AFM, atomic force microscopy; EMSA, electrophoretic mobility shift assay; IR, inverted repeat; MDR, multidrug resistance; OP-Cu, Cu-phenanthroline; $^{P}/_{O}$, promoter/operator; qPCR, quantitative PCR.

A supplementary figure and three supplementary tables are available with the online version of this paper.

repressor of the expression of the *lmrCD* genes. Most of the transcriptional regulators involved in MDR belong to the AraC, MarR, MerR and TetR families of transcriptional regulators. However, LmrR belongs to PadR, a family of mostly poorly characterized regulatory proteins that are involved in the regulation of detoxification mechanisms such as phenolic acid metabolism (Gasson *et al.*, 1998; Overhage *et al.*, 1999; Segura *et al.*, 1999). Apart from LmrR, LadR from *Listeria monocytogenes* is the only characterized member of the MDR-related PadR regulators (Agustiandari *et al.*, 2008; Huillet *et al.*, 2006). In this family of regulators, the expression of the detoxification genes is typically induced by the presence of the toxic compounds in the medium via a direct interaction with the PadR-like regulator. Indeed, LmrR has been shown to bind several of the LmrCD substrates, such as Hoechst 33342, daunomycin and sodium cholate. On the other hand, LmrR does not bind ρ-coumaric acid and ferulic acid (our unpublished data), which are the phenolic acid derivatives that have been shown to bind to PadR (Gury *et al.*, 2004). We have solved the structure of the LmrR dimer in the apo form and in two drug-bound forms, i.e. with Hoechst 33342 and daunomycin (Madoori *et al.*, 2009). The dimer contains two N-terminal DNA-binding domains with a typical winged helix–turn–helix (wHTH) motif, while the C-terminal regions form a large flat central pore at the subunit interface. The latter constitutes the drug-binding pocket of LmrR, which is symmetrical with equal contributions from both monomers to the overall structure. On the other hand, the exact induction mechanism of LmrR will only be determined when the crystal structure of LmrR bound to DNA is available. However, one possible mechanism of *lmrR* upregulation in the cell is via allosteric coupling between the drug- and DNA-binding sites, based on the comparison of different LmrR structures and the study of mutational analysis. The binding of the drug molecule to LmrR locks the dimer conformation in such a way that the DNA recognition helices fail to bind to their recognition site on the DNA major grooves (Madoori *et al.*, 2009).

The *lmrR* gene is located upstream of the *lmrCD* genes (Agustiandari *et al.*, 2008). In independently isolated drug-resistant strains of *L. lactis* that are cross-resistant against a series of drugs, the *lmrCD* genes are constitutively expressed because of the presence of defective forms of LmrR that are no longer able to bind to the promoter/operator ($^{P}/_{o}$) region of the *lmrCD* genes (Lubelski *et al.*, 2006). In these strains, the *lmrR* gene is also upregulated, suggesting that in wild-type cells, LmrR represses its own expression. Biochemical data demonstrate that LmrR indeed binds to its own promoter region (Agustiandari *et al.*, 2008). Here, we have analysed the interaction between LmrR and the control regions of the *lmrCD* and *lmrR* genes using 'in-gel' Cu-phenanthroline (OP-Cu) footprinting analysis and atomic force microscopy (AFM) imaging. The data suggest distinct modes of binding of LmrR to the *lmrR* and *lmrCD* control regions, resulting in the formation of different transcripts that encode the structural genes either with or without the *lmrR* transcriptional regulator gene. Expression of both *lmrR* and *lmrCD* is elevated when cells are grown in the presence of drugs, suggesting a mechanism in which the regulator gene and the functional genes are induced and co-transcribed from a polycistronic messenger.

METHODS

Protein purification. Strep-tagged LmrR protein was overexpressed in *L. lactis* NZ9000, and purified by strep-tag affinity chromatography followed by chromatography with a heparin column, as described previously (Agustiandari *et al.*, 2008).

Primer extension and RT-PCR analysis. RNA was extracted from *L. lactis* MG1363 using TRIzol reagent (Invitrogen). To prevent genomic DNA contamination, RNA samples were treated on-column with DNase I using an RNeasy Mini kit (Qiagen). Genomic DNA was extracted from *L. lactis* MG1363 using the GenElute Bacterial Genomic DNA kit (Sigma-Aldrich). Primer extension analysis was performed as described previously (Enoru-Eta *et al.*, 2002) using AMV Reverse Transcriptase (Roche Applied Science). The 5′ end-labelled primers DC620r or DC621r were used for transcription start determination of *lmrR* or *lmrC*, respectively. Labelling was done using [γ-^{32}]P-ATP (GE Healthcare). Reference ladders were generated by chemical sequencing methods (Maxam & Gilbert, 1980). cDNA was prepared from about 2 µg *L. lactis* RNA by using Superscript II Reverse Transcriptase (Invitrogen) and 200 ng random primers. This reaction was followed by RNase H treatment (Fermentas). Transcript analysis was done by PCR with primers Cdprmf/DC621r or DC636f/DC621r, using cDNA as template. Primer sequences are shown in Supplementary Table S1.

Electrophoretic mobility shift assays (EMSAs) and in-gel OP-Cu footprinting. Labelled DNA fragments were produced by PCR (ReadyMix *Taq* PCR Reaction Mix, Sigma-Aldrich) using a pair of primers, of which one was 5′ end-labelled with [γ-^{32}P]ATP (GE Healthcare). For the promoter regions of *lmrR* and *lmrCD*, the primer pairs DC634f/DC620r and DC635f/DC621r, respectively, were used with *L. lactis* MG1363 genomic DNA as template. Labelled fragments were purified by PAGE. The truncated fragments of the promoter regions of *lmrR* and *lmrCD* were prepared similarly using the set of primers listed in Supplementary Table S2. EMSAs were performed as described previously (Enoru-Eta *et al.*, 2000). Binding reactions were performed in LmrR binding buffer (20 mM Tris, pH 8.0, 1 mM $MgCl_2$, 20 mM KCl, 0.1 mM DTT, 0.4 mM EDTA, 12.5 %, v/v, glycerol) by incubating at 37 °C for 30 min in the presence of 25 µg ml^{-1} sonicated herring sperm DNA as a non-specific competitor. K_D values were estimated based on these EMSAs, as the protein concentration at which about 50 % of the DNA was bound (expressed in dimer equivalents). In-gel OP-Cu footprinting was performed as described previously (Peeters *et al.*, 2004). Reference ladders were generated by chemical sequencing methods (Maxam & Gilbert, 1980).

AFM. For AFM experiments, the DNA fragments were prepared by PCR with ReadyMix *Taq* PCR Reaction Mix (Sigma-Aldrich). The $^{P}/_{o}$ region of *lmrR* was amplified as a 997 bp fragment with the primer pair AFM *lmrR* pmtr FW/AFM *lmrR* pmtr RV, and *L. lactis* MG1363 genomic DNA as template. A 1016 bp fragment containing the $^{P}/_{o}$ region of *lmrCD* was amplified with the primer pair AFM *lmrCD* pmtr FW/AFM *lmrCD* pmtr RV. Following PCR amplification, all fragments were purified by agarose gel electrophoresis using a GenElute Gel Extraction kit (Sigma-Aldrich). A number of trials were performed to find the best concentration for both DNA and LmrR, with final concentrations of 1.86 and 0.04 µM for *lmrR* DNA and LmrR

protein, respectively; and 0.16 and 0.018 μM for *lmrCD* DNA and LmrR protein, respectively. These binding reactions were diluted in LmrR binding buffer in a total volume of 15 μl. The mixture was then diluted twofold in adsorption buffer (40 mM HEPES, pH 6.9, 10 mM $NiCl_2$), and 15 μl of the suspension was deposited on freshly cleaved mica. This was incubated for 5 min to allow adsorption of the nucleoprotein complexes. Subsequently, samples were rinsed with deionized ultrapure water and excess water was blotted off with absorbent paper. The mica surface was blown dry in a stream of filtered air. A NanoScope IIIa atomic force microscope (Digital Instruments/Veeco) was operated in the tapping mode, in air. Images of 512 × 512 pixels were acquired by using Nanoprobe scanning probe microscopy (SPM) tips, type RTESP7 (Veeco) with a 115–135 μm cantilever, a nominal spring constant of 50 N m^{-1} and resonance frequencies in the range from 244 to 295 kHz. The scan size was 1.5 μm × 1.5 μm and the scan rate was 2 Hz. NanoScope 6.11r1 software (Digital Instruments/Veeco) was used to flatten the images and to make zoomed 3D surface plots. The contour lengths of DNA molecules or DNA arms of complexes were measured by manual tracing with ImageJ (Abramoff *et al.*, 2004). DNA molecules or complexes with overlapping parts or with visible anomalies were omitted from the analysis.

Quantitative PCR (qPCR). Cultures of *L. lactis* NZ9000 and NZ9000(Δ*lmrR*) (Agustiandari *et al.*, 2008) were grown overnight on M17 supplemented with 0.5 % glucose at 30 °C. Cultures were diluted 1 : 100 to an OD_{660} of 0.07–0.08 in the same medium with or without 1 μM Hoechst 33342 (Sigma-Aldrich) or 20 μM daunomycin (Calbiochem – VWR). These subinhibitory drug concentrations ensured near-identical growth rates of the different types of cells. Cells were further grown at 30 °C, and during the early exponential, late exponential and stationary growth phases, samples of 5 ml were collected and flash-frozen in liquid nitrogen. Total RNA was isolated using TRIzol reagent (Zaidi *et al.*, 2008). Residual chromosomal DNA was removed by using the TURBO DNA-*free* kit (Ambion, Applied Biosystems) according to the manufacturer's instructions. Purified RNA was quantified by measuring A_{260} using a NanoDrop ND1000 spectrophotometer. The quality of the RNA preparations was checked by visualizing the integrity of 16S and 23S rRNA on an agarose gel, and by verifying the absence of DNA contamination by PCR. The cDNA molecules were synthesized using an iScript cDNA synthesis kit (Bio-Rad) as recommended by the manufacturer. Total RNA was isolated from at least two separately grown replicate cultures.

For the qPCR experiments, the primers were designed to have a length of 22–23 nt, a G/C content of 45–47 % (see Supplementary Table S3) and a T_m of about 60–65 °C. The lengths of the primer products ranged between 200 and 230 bp. qPCR was carried out on a MiniOpticon Real-Time PCR system (Bio-Rad). After dilution of the cDNA, 4 μl was added to 21 μl of the PCR mixture (12.5 μl iQ SYBR Green Supermix and 0.5 μl of each primer at 10 pmol μl^{-1}). Thermal cycling conditions were as follows: initial denaturation at 95 °C for 3 min, followed by 40 cycles of 95 °C for 20 s, 55 °C for 20 s and 72 °C for 30 s. An additional step starting from 65 to 95 °C was performed to establish a melting curve. This was used to verify the specificity of the PCR for each primer set. qPCR measurements were performed in duplicate for each sample. The *tufA* gene was used as an internal control and for normalization of the results (Friedrich & Lenke, 2006).

RESULTS

Mapping of the transcription start sites of *lmrCD* and *lmrR*

Primer extension analysis was performed to map the transcription initiation sites of the *lmrCD* and *lmrR* genes using RNA extracted from *L. lactis* MG1363 cells (Fig. 1). Transcription of *lmrR* is initiated at a single G residue located 26 nt upstream of the ATG start codon (Figs 1a and 2a). In contrast, *lmrCD*-specific reverse transcription resulted in at least four different cDNA molecules (Figs 1b and 2b). Transcripts C and D start at an A residue 55 and 61 nt upstream of the ATG start codon of *lmrC*, respectively. Transcript B starts at a T residue that is located 100 bp upstream of the ATG start codon of LmrC. A fourth cDNA molecule represents a transcript that is larger than the labelled fragment used for the Maxam–Gilbert sequencing ladder, which was prepared by PCR amplification using primers CDprmf and DC621r (Fig. 1d, Supplementary Table S1). Therefore, this transcript must also contain at least part of the ORF of *lmrR*. To test whether or not this transcript corresponded to transcript A as detected by *lmrR*-specific primer extension, RT-PCR analysis was performed using primer pairs CDprmf/DC621r and DC636f/DC621r (Fig. 1c, d). These reactions resulted in amplification, confirming the existence of an mRNA molecule that spans both the *lmrR* gene and the *lmrCD* gene. It thus appears that an RNA polymerase initiated at the *lmrR* promoter may proceed till the end of *lmrD*. Indeed, using the program TransTerm, intrinsic terminators were predicted to occur neither in the *lmrR* and *lmrCD* genes nor in the intergenic region between *lmrR* and *lmrC*, although a terminator was detected downstream of *lmrD*. Putative Shine–Dalgarno (SD) sequences for both *lmrR* and *lmrC* were detected between the seventh base and the twelfth base upstream of the respective start codons. Regions that showed sequence conservation with the consensus −35 and −10 promoter elements could be identified slightly upstream of the start of transcripts A and B (Fig. 2a, b). Both promoters showed a putative Pribnow box with a perfect match to the consensus and a −35 sequence with a good match, the two being separated by a linker of ideal length (17 bp). However, in view of the multiple transcripts observed for *lmrCD*, additional promoter element(s) might be involved in *lmrCD* expression, although it cannot be excluded that these transcripts may arise by degradation of the longer transcripts.

Identification of the LmrR-binding sites in the control regions of *lmrR* and *lmrCD*

Previously, it has been shown that LmrR protects a long stretch of DNA in the control region of its own gene against DNase I (Agustiandari *et al.*, 2008). Here, we show that LmrR forms multiple complexes with $^{P}/_{o}$ *lmrR* DNA as observed in an EMSA (Fig. 3a). This result suggests the presence of multiple binding sites that likely involve several copies of LmrR. Three complexes (B1, B2 and B3) showed a slightly different migration velocity, whereas complex B4, which was detected only at the highest LmrR concentration used (0.8 μM), was strongly retarded in its mobility. The average apparent binding dissociation constant (K_D) of the LmrR–$^{P}/_{o}$ *lmrR* interaction was around 30 nM. There was a

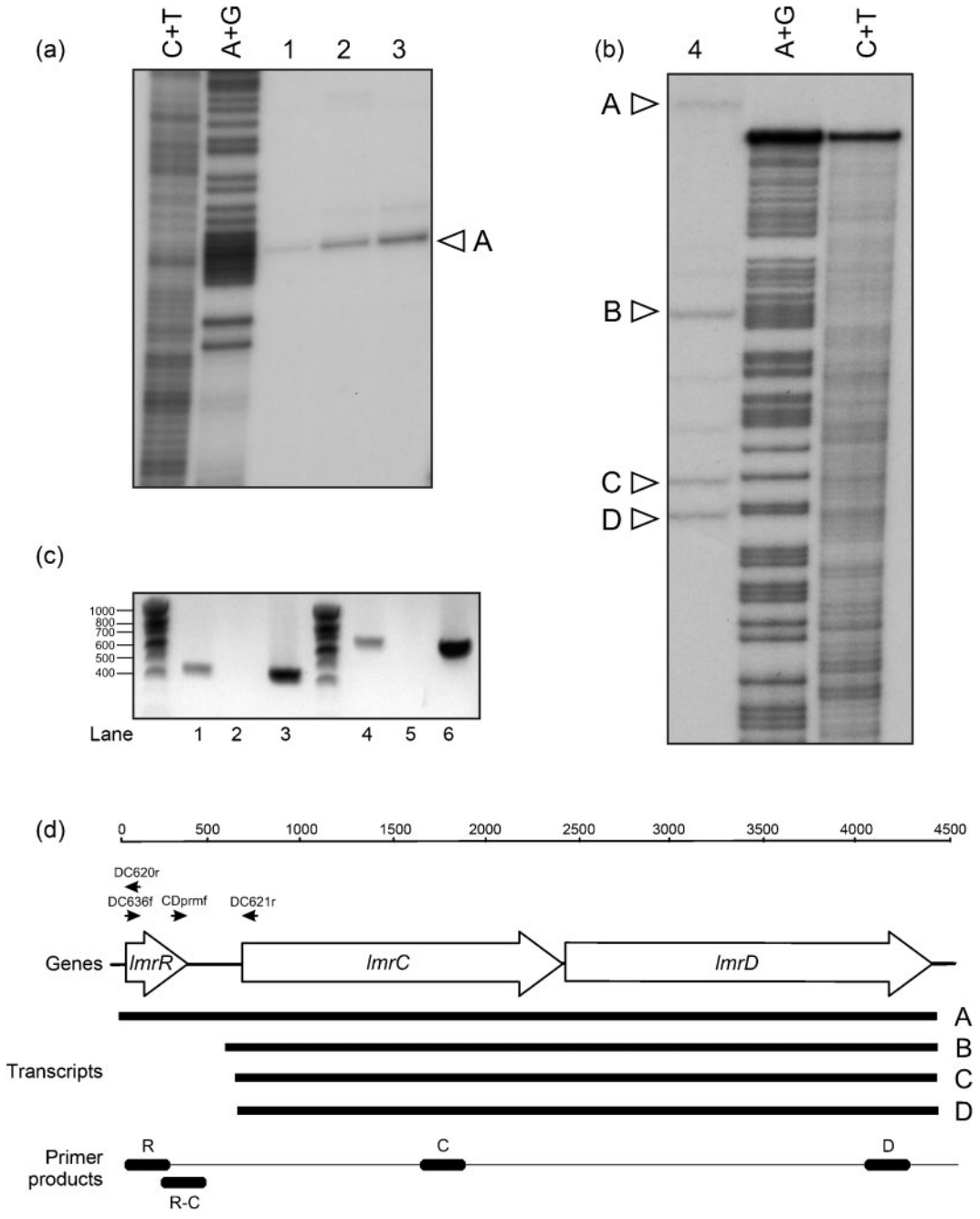

Fig. 1. Primer extension analyses of transcripts showing the transcription start sites of (a) *lmrR* using primer DC620r and (b) *lmrC* using primer DC621r. The amounts of total RNA used were 12.5 μg (lane 1), 25 μg (lane 2), 50 μg (lane 3) and 100 μg (lane 4). The main primer extension products are indicated with arrowheads and are designated A to D. A+G and C+T represent the corresponding Maxam–Gilbert sequencing ladders. A systematic correction in the alignment of the cDNA product with the sequencing ladders has been performed to take into account the difference in migration velocity of the cDNA and the reference ladders due to different ends generated by the AMV reverse transcriptase and the chemical modification and cleavage reactions. (c) RT-PCR analysis with cDNA as template with primers CDprmf and DC621r (lane 1); as lane 1, without addition of reverse transcriptase (negative control) (lane 2); with primers CDprmf and DC621r and with genomic DNA as template (lane 3); with primers DC636f and DC621r and with cDNA as template (lane 4); as lane 4, but without addition of reverse transcriptase (negative control) (lane 5); with primers DC636f and DC621r and with genomic DNA as template (lane 6). (d) Schematic overview of the transcripts A, B, C and D with respect to the ORFs (indicated with open arrows) and primer products used for qPCR. The locations of the primers used for primer extension and RT-PCR analysis are also indicated.

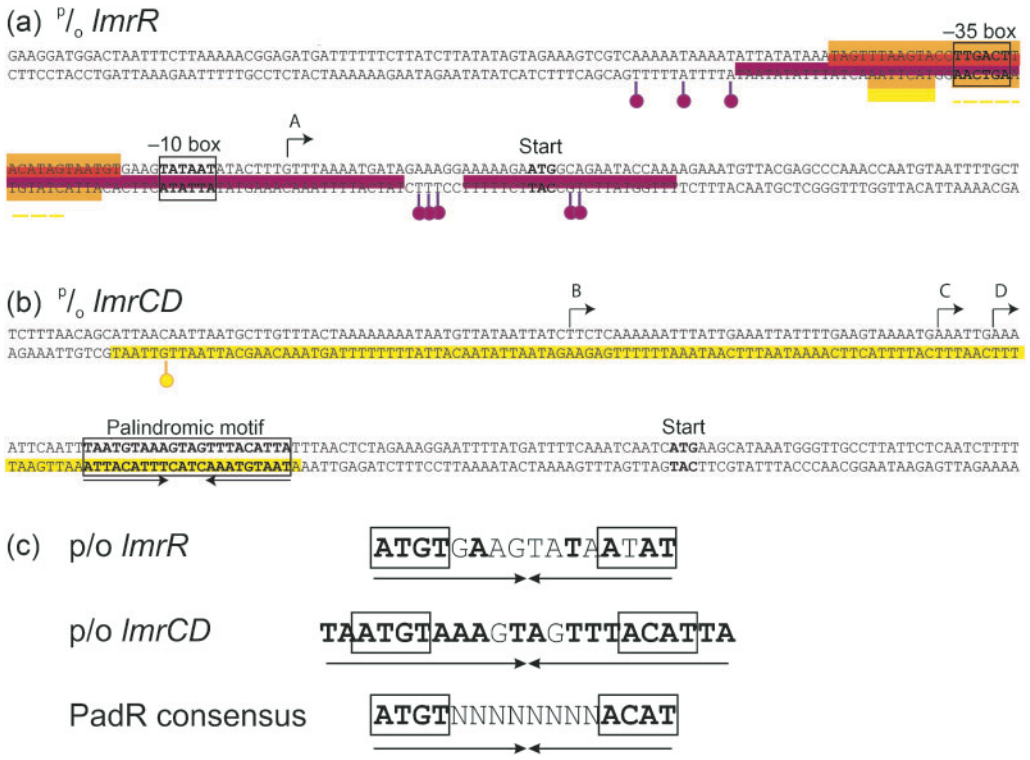

Fig. 2. Schematic representation of the transcriptional elements on (a) *lmrR* and (b) *lmrCD* control region DNA, including the positions of the −35 and −10 regions, the transcription initiation sites, and the translation start codon (bold type). For the promoter region of *lmrCD*, the predicted promoter elements are only shown for transcript B. The letters A to D represent the 5′ end of the major transcripts observed in primer extension analysis. In addition, the protected areas observed in the footprinting assays of LmrR binding to $P/_o$ *lmrR* (A) and $P/_o$ *lmrCD* (B) are shown. For $P/_o$ *lmrR*, protection zones are indicated for the complexes B1 (yellow), B2 (orange), B3 (red) and B4 (purple). For $P/_o$ *lmrCD*, the protection zone is indicated in yellow. The ball-and-stick symbols represent the positions of the hyper-reactivity sites. The identified imperfect palindromes are shown in the sequences with double arrows. (c) Representation of the imperfect IRs as identified in $P/_o$ *lmrR*, $P/_o$ *lmrCD* and the PadR consensus IR. Palindromic residues are in bold type, and the conserved PadR motif is boxed.

rapid transition in the formation of the different complexes, which suggested cooperativity in the binding. EMSAs were also performed with truncated DNA fragments containing only a part of the *lmrR* control region or ORF (Fig. 3b, c). Interestingly, LmrR was able to bind DNA probes consisting of the control region alone (Rtrunc1 and Rtrunc2), and also a DNA probe consisting mainly of the *lmrR* gene, starting only 4 bp upstream of the transcription start (Fig. 3c) (Rtrunc3). However, although the Rtrunc2 and Rtrunc3 fragments were of nearly identical length, the LmrR–Rtrunc3 complex migrated differently and was less stable, indicative of a different architecture and/or stoichiometry of this complex. These binding events were specific, since no complex formation was observed under identical conditions with a DNA fragment corresponding to the region upstream of the −35-promoter element of *lmrC* (Supplementary Fig. S1).

To further determine which regions of the DNA are recognized by LmrR in each of the multiple complexes observed in the EMSA, in-gel OP-Cu footprinting was performed with the various complexes (Fig. 3d). A stretch of 6 nt was clearly protected in the fastest-migrating complex B1 (Fig. 2a, yellow bar, and Fig. 3d). This initially protected site might be considered as a 'core'-binding binding site from which LmrR binding is nucleated. In addition, a difference in the cleavage pattern, between on the one hand the complexed B1 form and on the other hand the free I and F forms, could be observed in an approximately 13 nt long region, immediately downstream of this stretch (Fig. 2a, yellow dashed bar, and Fig. 3d). This stretch, including the −35 box, is part of a region that is much more clearly protected in complexes B2 and B3 (Fig. 2a, orange and red bars). Footprinting with a DNA fragment with the top strand labelled revealed no clear-cut differences in the protected regions of complexes B2 and B3. This might be explained by (i) a slightly different architecture of the complex, (ii) a different stoichiometry of the complex without supplementary DNA contacts, or (iii) the formation of a 'sandwich-like' structure containing two DNA molecules. The highly retarded complex B4 showed extensive protection encompassing about 102 bp,

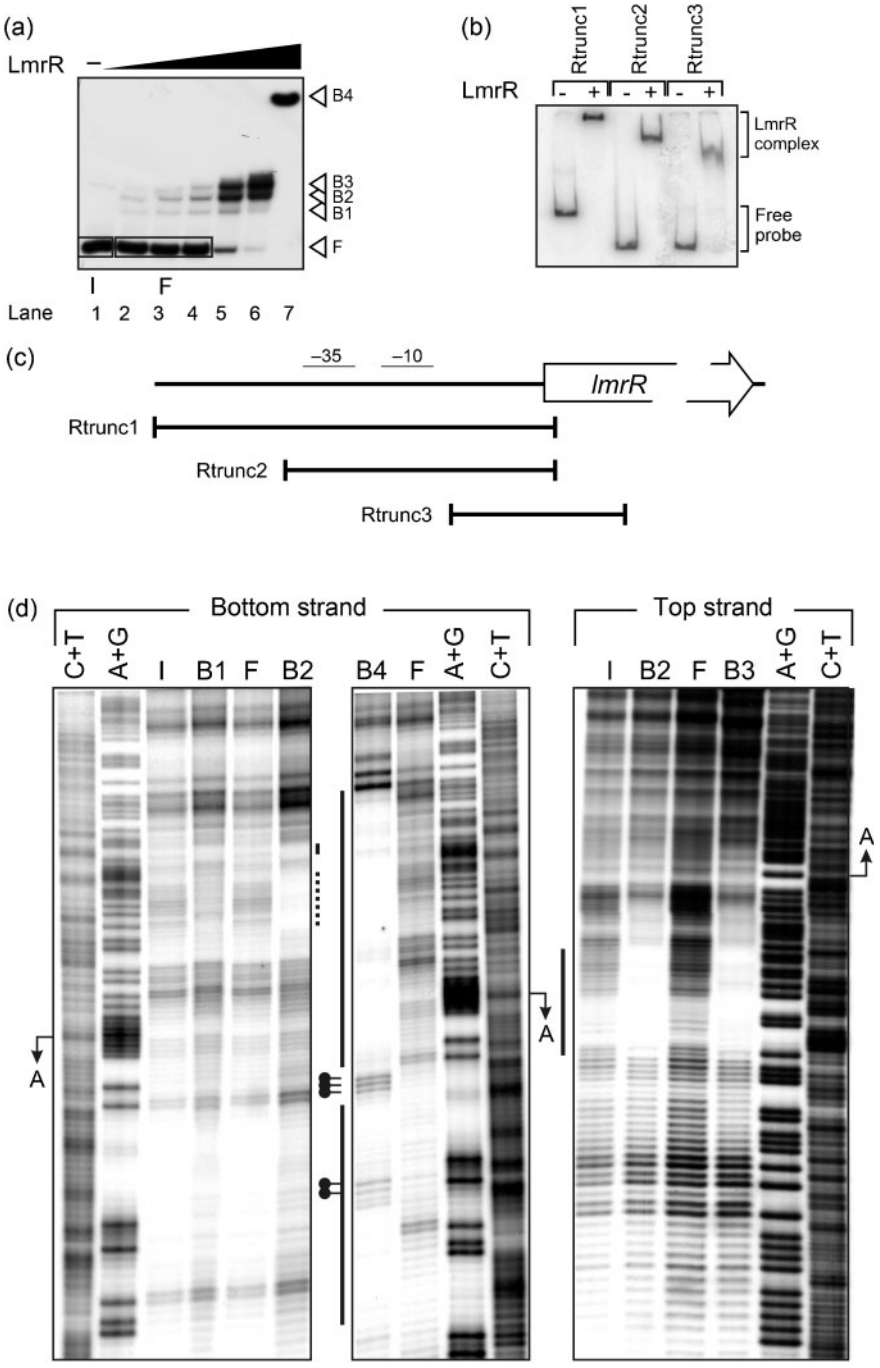

Fig. 3. Binding of LmrR to the *lmrR* $^{P}/_{o}$ region. (a) EMSA of the binding of purified LmrR to a 210 bp labelled DNA fragment containing the *lmrR* $^{P}/_{o}$ region. The LmrR stock concentration was 81.5 μM (dimer) and was further diluted. No LmrR was added in lane 1, and LmrR was added at concentrations of 0.01 μM (lane 2), 0.02 μM (lane 3), 0.03 μM (lane 4), 0.1 μM (lane 5), 0.2 μM (lane 6) and 0.8 μM (lane 7). The positions of the free DNA (F) and of the different LmrR-bound DNA complexes (B1, B2, B3 and B4) are indicated. These different complexes and the boxes named I (input DNA) and F (free DNA) were excised for in-gel footprinting analysis. (b) EMSA of the binding of purified LmrR to truncated DNA fragments Rtrunc1 (266 bp), Rtrunc2 (170 bp) and Rtrunc3 (152 bp), corresponding to the regions of the *lmrR* operator site indicated in Fig. 2. LmrR was added at a final concentration of 1.85 μM (dimer). (c) Schematic of the coverage of the $^{P}/_{o}$ *lmrR* truncated fragments Rtrunc1, Rtrunc2 and Rtrunc3 relative to the *lmrR* promoter elements and ORF. (d) In-gel OP-Cu footprinting of LmrR binding to the $^{P}/_{o}$ region of *lmrR* with the bottom strand labelled (left two panels) or with the top strand labelled (right panel). The EMSA that was used for the experiment with the bottom strand labelled is shown in Fig. 3(a). Next to each autoradiograph, protected regions are indicated with a vertical line. Hyper-reactivity sites are also indicated with ball-and-stick symbols. For the far-left panel, the full line

corresponds to protection observed in complexes B1 and B2, whereas the dashed line corresponds to additional protection observed in complex B2 alone. A+G and C+T represent the Maxam–Gilbert sequencing ladders. Next to the ladder, the position of the transcription start is shown. A schematic representation of the protected regions is displayed in Fig. 2.

including the entire promoter and transcription start site (Fig. 2a, purple bar, and Fig. 3d). In this protected region, an imperfect inverted repeat (IR) is apparent (Fig. 2a, c). This IR exhibited one mismatch as compared with the PadR consensus sequence, but had the optimal spacing of 8 nt between the palindromic half sites (Fig. 2c) (Huillet *et al.*, 2006). Several hyper-reactivity signals were observed for complex B4, indicating local DNA deformations (minor groove widening) upon LmrR binding (Figs 2a and 3d).

The binding of LmrR to DNA fragments covering the $^{P}/_{o}$ region of the *lmrCD* genes showed a distinctively different signature. Previous footprinting results had indicated that LmrR binds to two different sites on the *lmrCD* promoter (Agustiandari *et al.*, 2008): site I, comprising the −35 and −10 regions, and site II, which harbours an imperfect IR similar to the PadR consensus sequence but with a spacing of 10 bp (Fig. 2c) (Huillet *et al.*, 2006). EMSAs were performed with shortened probes corresponding to either site I or site II (Supplementary Fig. S1). It appeared that LmrR bound DNA probes containing the −35 and −10 regions (site I) more strongly than the probes containing site II with the palindromic sequence. With the full-length *lmrCD* $^{P}/_{o}$ DNA, a major specific complex was observed upon binding of LmrR (Fig. 4a). The overall binding affinity of this interaction appeared to be two- to fourfold lower than the affinity for $^{P}/_{o}$ *lmrR* DNA, with an apparent K_D of about 150 nM. In-gel OP-Cu footprinting of LmrR binding to the *lmrCD* control region showed a single extended protected region of about 126 bp (Fig. 4b) that overlapped all the transcription initiation sites (site I) in the *lmrCD* control region and their cognate promoter elements, and the previously identified imperfect IR (site II; Fig. 2b). At the promoter-distal side of the protected region, a hyper-reactivity site was observed, again indicating LmrR-induced DNA deformations. These results demonstrate different modes of binding of LmrR to the *lmrR* and *lmrCD* $^{P}/_{o}$ regions.

AFM of the binding of LmrR to *lmrR* and *lmrCD* promoter DNA

AFM was used to visualize the architecture of LmrR complexes formed with the $^{P}/_{o}$ regions of *lmrR* and *lmrCD* (Figs 4c and 5). Tapping-mode AFM in air was used for high-resolution topographic imaging of the soft protein/DNA sample surfaces without creating destructive frictional forces. With the *lmrR* $^{P}/_{o}$ DNA, 22 unbound 997 bp-long DNA molecules and 41 DNA–LmrR complexes were analysed. The contour length of unbound DNA molecules was manually traced using ImageJ software, resulting in a mean contour length of 313 nm (SD 29 nm; Fig. 5c). This yielded an axial basepair rise of 0.31 nm bp^{-1}, which is slightly lower than the theoretical rise of B-form DNA (i.e. 0.34 nm bp^{-1}), but in good agreement with other AFM studies. This difference can be explained by the limited resolution of the microscope and the smoothing procedure that rounds sharp bends (Rivetti *et al.*, 1996). Based on DNA persistence length analysis of other DNA molecules measured under similar experimental conditions, it can be assumed that the molecules are able to freely equilibrate on the surface before capture (Peeters *et al.*, 2006; Minh *et al.*, 2009).

A heterogeneous population of LmrR–*lmrR* nucleoprotein complexes was observed, ranging from having apparently a single site bound, possibly the 'core' nucleation site (Fig. 5a, images 1–3), to having apparently two sites bound or even large complex regions. Here, several LmrR molecules seemed to be involved in the condensation of the binding site area (Fig. 4c, image 4). This type of complex most probably corresponds to the B4 population observed in the EMSA (Fig. 3a). It is clear that LmrR binding induces severe DNA deformations, including sharp DNA bending, DNA condensation and possibly even DNA wrapping around the protein (local constrained toroidal DNA supercoiling) or DNA looping (Fig. 5a). The contour length of the naked DNA arms of all complexes was measured without making a distinction between the different types of complexes (depending on the degree of binding; Fig. 5b). These measurements resulted in a mean length of 79 nm (SD 39 nm) for the short DNA arm and 191 nm (SD 40 nm) for the long DNA arm. Therefore, the total mean visible contour length of the complexes (short + long arms) was 270 nm (SD 52 nm; Fig. 5c). This is a difference of 43 nm from that of the mean length of the unbound DNA molecules, and taking a basepair rise of 0.31 nm bp^{-1} into account, this corresponds to about 139 bp condensed inside the DNA–LmrR complex. Due to the heterogeneity of the complexes, the distributions are broad. These observations demonstrate that the mechanism of binding of LmrR to the *lmrR* $^{P}/_{o}$ DNA involves interactions with multiple LmrR molecules that are likely bound in a cooperative fashion. Furthermore, the extent of the condensation is in good agreement with the length of the protected region as observed for complex B4 in in-gel OP-Cu footprinting.

AFM experiments with the *lmrCD* control region DNA resulted in LmrR–DNA complexes with a more homogeneous architecture than that of the LmrR–$^{P}/_{o}$ *lmrR* complexes (Fig. 4c). The results indicated that LmrR induces a significant DNA bending. Typically, the complexed region had a bilobed structure. The two 'blobs' present in the AFM images may represent the

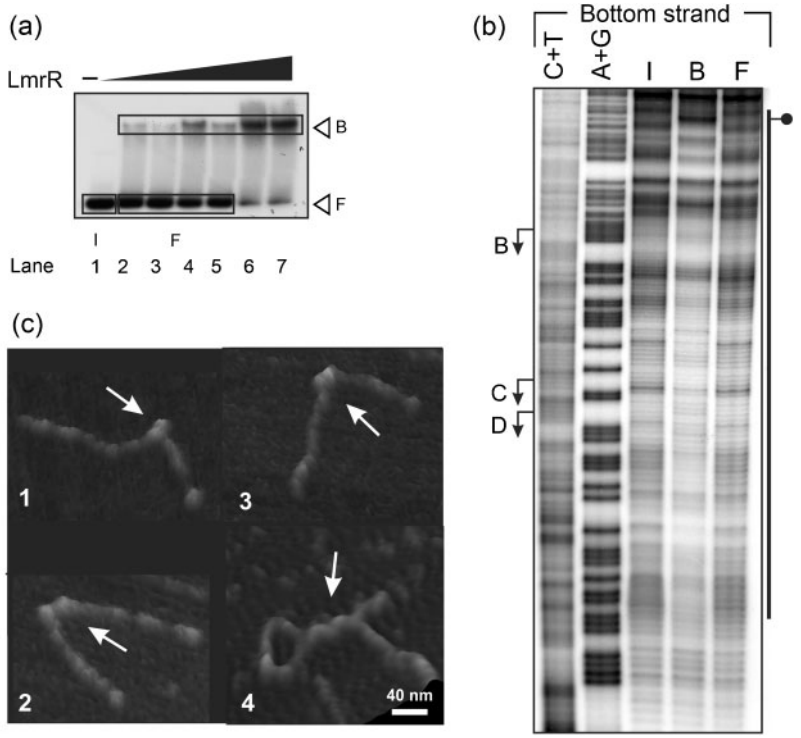

Fig. 4. Binding of LmrR to the *lmrCD* $^{P}/_{o}$ region. (a) EMSA of the binding of LmrR to a DNA fragment corresponding to the *lmrCD* $^{P}/_{o}$ region. No LmrR was added in lane 1, and LmrR was added at concentrations of 0.01 μM (lane 2), 0.02 μM (lane 3), 0.03 μM (lane 4), 0.1 μM (lane 5), 0.2 μM (lane 6) and 0.8 μM (lane 7). The positions of input (I), free DNA (F) and bound complexes (B) are indicated. (b) In-gel OP-Cu footprinting analysis of the LmrR–*lmrCD* promoter region complex that was excised from the gel shown in Fig. 3(b). Next to the autoradiograph, the protected regions are indicated with a vertical line and the hyper-reactivity sites as a ball-and-stick symbol. A+G and C+T represent the Maxam–Gilbert sequencing ladders. Next to the ladder, the positions of the transcription starts are shown. A schematic representation of the protected region is displayed in Fig. 2. (c) A selection of AFM images of LmrR–$^{P}/_{o}$ *lmrCD* protein–DNA complexes (indicated by the arrows), as typically observed.

binding of two LmrR dimers to the DNA (Fig. 4c) (Madoori *et al.*, 2009). Taken together, the AFM results support the notion that LmrR binds the *lmrR* and *lmrCD* operator regions by different mechanisms, and indicate higher-order interactions of LmrR with the operator region of its own gene.

Expression analysis of the *lmrCD* and *lmrR* genes in *L. lactis*

Our analysis indicated the presence of a long transcript harbouring both the *lmrR* gene and the *lmrCD* gene. To assess the expression levels of *lmrR* in growing cell cultures, qPCR was employed on RNA extracted from *L. lactis* cells

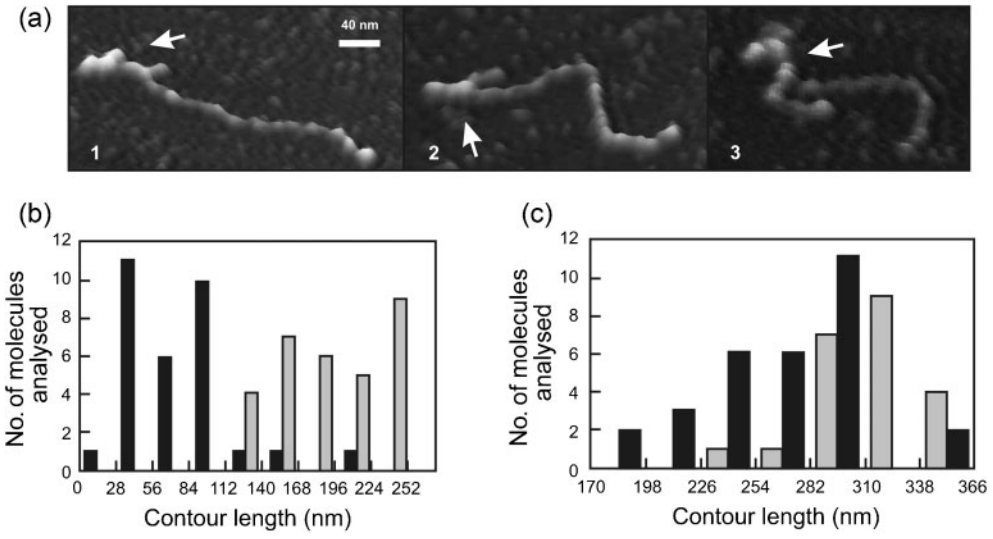

Fig. 5. AFM analysis of the binding of LmrR to the $^{P}/_{o}$ site of *lmrR*. (a) A selection of AFM images of LmrR–$^{P}/_{o}$ *lmrR* protein–DNA complexes (indicated by the arrows). (b) Contour length measurements of the long (grey bars) and short (black bars) arms of LmrR complexed with the DNA fragment. (c) Contour lengths of the sum of the long and short arms of the LmrR-complexed DNA fragments (black bars) and of the free DNA fragments (grey bars). The *y* axes indicate the number of analysed molecules.

growing on M17 medium with glucose in the absence and presence of subinhibitory concentrations of the drugs daunomycin and Hoechst 33342. As a control, *L. lactis* NZ9000(Δ*lmrR*) was used, which expresses the *lmrCD* genes constitutively (Agustiandari *et al.*, 2008). Primer sets were designed to monitor the transcript levels of *lmrR*, *lmrC* and *lmrD* individually, and in addition, a set was designed that detected the intergenic region that separates the *lmrR* and *lmrCD* genes in the long polycistronic *lmrR–lmrCD* transcript (Fig. 1d). Expression levels were related to that of the housekeeping gene *tufA*, which encodes the translation elongation factor Tu (Friedrich & Lenke, 2006). In addition, the *secY* transcript, encoding the major subunit of the preprotein translocase, was monitored. The expression level of these control genes was constant during exponential growth, but unlike *tufA*, the expression of *secY* dropped when cells entered the stationary phase (Fig. 6). As expected, the *lmrC* and *lmrD* genes were highly expressed in *L. lactis* NZ9000(Δ*lmrR*) cells during the exponential and stationary growth phases. With *L. lactis* NZ9000 wild-type cells, lower levels of *lmrCD* expression were observed that dropped dramatically when the cells entered the stationary phase. A similar response was observed with the transcript containing the *lmrR* gene and the *lmrR–lmrC* intergenic region, suggesting that the long transcript is present during the entire exponential growth phase. When cells were exposed to daunomycin (Fig. 6) or Hoechst 33342 (data not shown), expression levels of *lmrC* and *lmrD* increased. Since Hoechst 33342 also caused an increase in *tufA* expression, the corresponding data could not be quantified. Remarkably, exposure to the drugs also resulted in increased levels of the transcript harbouring the *lmrR* gene and the *lmrR–lmrC* intergenic region. Summarizing, these data demonstrate that both the regulatory *lmrR* gene and the structural *lmrCD* genes are expressed in exponentially growing wild-type cells and that their expression increases upon exposure to toxic drugs.

DISCUSSION

The ABC transporter LmrCD has previously been shown to be a major determinant of the MDR phenotype in *L. lactis* (Lubelski *et al.*, 2006). Transcription of *lmrCD* is controlled by LmrR, a local regulatory repressor whose gene is located upstream of *lmrCD* (Agustiandari *et al.*, 2008). The *lmrR* and *lmrCD* genes are transcribed in the same direction. LmrR has previously been shown to function as a drug-controlled negative transcriptional regulator of the expression of the *lmrCD* genes. Our current primer extension analysis now reveals the presence of three major transcripts of *lmrCD*, and one longer transcript spanning the *lmrR* and *lmrCD* genes. The occurrence of multiple transcripts of *lmrCD* might indicate the presence of alternative promoters. Alternative promoters are quite frequent in bacteria and may be used to cope with changes in the environment, such as altered nutritional requirements that result in changes in the expression of a particular gene. In most cases, however, one promoter is responsible for constitutive expression, while the others are inducible by different stimuli (Musso *et al.*, 1977) and may even function with another alternative sigma factor. At this stage it is unclear whether the presence of these multiple transcripts indeed reflects functional differences in the regulation and/or expression mechanism. Possibly, additional global or local regulators are involved in the regulation of the different promoters. However, qPCR analysis of the expression of *lmrR* (from the long transcript) and of the *lmrCD* genes (likely both from the long and shorter transcripts) indicated that these genes are expressed throughout the exponential growth phase, and that their expression is further elevated when cells are exposed to toxic drugs. For *lmrCD*, the drug-induced expression levels were lower than those observed in the deregulated strain that lacked the *lmrR* gene, indicating that the drug-induced derepression is not maximized in such cells.

LmrR binds to two regions in the *lmrCD* operator sequence. Site I, comprising the −35 and −10 region leading to initiation at transcription start site B, appears to be a high-affinity binding site for LmrR. Site II harbours an imperfect IR that is similar to the PadR consensus binding site, although the two half-sites are separated by 10 instead of 8 bp (Huillet *et al.*, 2006). EMSA data suggested that the palindromic sequence on its own is only weakly recognized by LmrR (Supplementary Fig. S1), and that the binding of LmrR to the entire control region of the *lmrCD* genes results in one dominant species of DNA–protein complex. In-gel footprinting analysis supported the notion that in this complex, both site I and site II are protected by LmrR. Visualization of these protein–DNA complexes by AFM revealed a significant DNA bending, with two protein 'blobs' present on the DNA, wherein each 'blob' likely corresponds to one LmrR dimer. Taken together, these results suggest that site I and site II are each bound by an LmrR dimer in a highly cooperative manner, since it was not possible to detect a complex with only the higher-affinity site I bound. On the other hand, an EMSA with LmrR binding to the control region of its own gene revealed the formation of several distinct complexes. In-gel footprinting revealed that in this control region, multiple copies of the LmrR protein bind and that this is a sequential event, nucleated by binding to a site just upstream of the −35 box and extending further downstream, overlapping the promoter and transcription initiation site, and spreading into the *lmrR* ORF. A PadR-like imperfect IR is located in the middle of this large protected zone, and might be recognized by LmrR. This binding seems to involve a cooperative mechanism in which protein–protein interactions between adjacently bound LmrR dimers and DNA conformational changes play an important role. It yields a higher-order multimeric LmrR–DNA complex in which the DNA is condensed, looped or even wrapped around the protein, as suggested by the AFM observations. Earlier observations describing the cooperative binding of two dimers of the λ repressor to

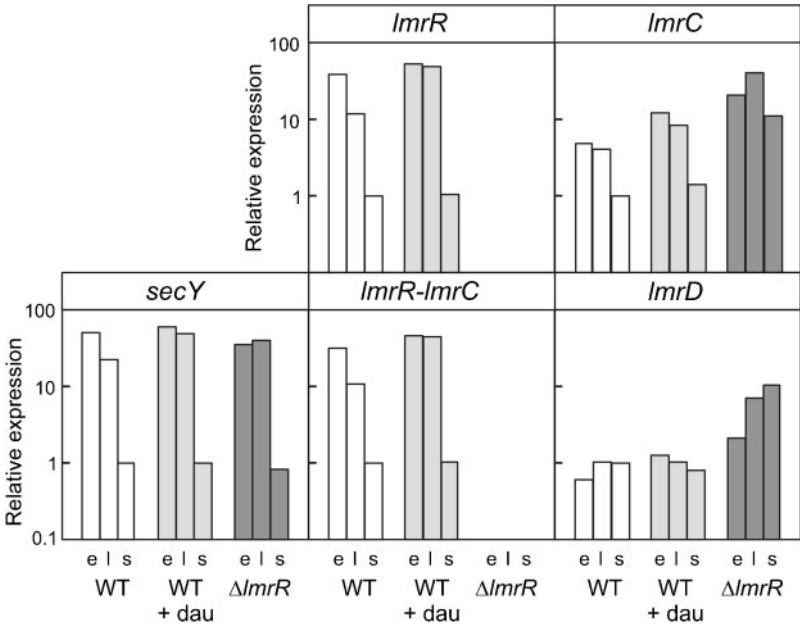

Fig. 6. qPCR expression analysis of *lmrCD*, *lmrR* and the intergenic region that separates the *lmrR* and *lmrC* genes in *L. lactis* NZ9000 (WT; white bars) cells grown to different growth stages in the absence and presence of daunomycin (dau; light-grey bars). *L. lactis* NZ9000(Δ*lmrR*) cells (dark-grey bars) were included as a control. Expression levels were related to those of elongation factor Tu (*tufA*), and normalized for each gene to the expression in the stationary phase of *L. lactis* NZ9000 cells in the absence of daunomycin. *secY* was used as an additional housekeeping gene. The efficiency of amplification reactions was determined by running a standard curve with serial dilutions of cDNA. PCR efficiencies were similar for the various primer sets and were above 95 %. Growth phases: e, early exponential; l, late exponential; s, stationary.

different and adjacent operator sites in the same DNA molecule have shown that this is mediated by the interactions between the carboxyl domains of the repressor molecules, which encourage the DNA to twist and bend due to its flexibility (Hochschild & Ptashne, 1986). Moreover, the binding of the repressor to a strong binding site will enhance the binding affinity of a weaker site, thus promoting cooperative binding between repressor molecules as described above. The same mechanism may apply for the binding of LmrR to the two different sites in the *lmrCD* operator region. Overall, our data suggest that the mechanisms by which LmrR binds to the control regions of the *lmrCD* and *lmrR* genes are different, with binding to $^{P}/_{o}$ *lmrR* occurring in a tighter fashion and with a higher binding affinity.

Based on our new insights, the following two-step mechanism of *lmrCD* regulation is envisaged (Fig. 7). Binding of two LmrR dimers to the *lmrCD* promoter region will result in a repression of *lmrCD* expression. Simultaneously, extensive binding of multiple LmrR dimers to the *lmrR* control region leads to a strong autorepression and repression of the *lmrCD* expression from the long transcript. When cells are challenged with toxic compounds, the drugs enter the cell and bind to LmrR. At first, this likely only causes a reduced binding of LmrR to the *lmrCD* operator binding sites. Consequently, there is a derepression of *lmrCD* transcription. At higher drug concentrations, the repression at the *lmrR* operator site might also be relieved, since this is a higher-affinity binding involving more LmrR dimers that interact tightly with each other and with the strongly deformed DNA. This derepression yields a polycistronic messenger containing the information for the regulator and for the transporter, resulting in an even higher production of LmrCD. Therefore, LmrR-mediated regulation of *lmrCD* expression is exerted from two different locations and by different mechanisms. Meanwhile, LmrR is also involved in an autorepression that is modulated by drugs. Only upon release of LmrR from the *lmrR* operator site (at high intracellular drug concentrations) is additional LmrR regulatory protein produced. These additional regulatory protein molecules may ensure a fast response to re-repress *lmrR* and *lmrCD* expression, as most LmrR dimers are already saturated with the drug effector molecule. Newly synthesized LmrCD will insert into the membrane and mediate the export of the drugs from the cell. Due to the decreased cellular drug levels, LmrR will return to its apo form and reassociate first with $^{P}/_{o}$ *lmrR* and then with the *lmrCD* operator site and again inhibit expression. This drug-dependent regulatory phenomenon results in a fine-tuned demand-dependent expression of the LmrCD transporter.

In the previously studied MDR strains, the *lmrR* gene harbours mutation(s) that lead to the production of non-functional LmrR variants that are unable to repress the expression of either *lmrR* or *lmrCD* (Agustiandari *et al.*, 2008). This causes not only the upregulation of *lmrCD* but also increased levels of the *lmrR* transcript. Strikingly, microarray analysis of all four drug-resistant strains of *L. lactis* demonstrated that *lmrR* is significantly and more strongly (mean 9.4-fold) upregulated than *lmrCD* (mean 6.7-fold) (Lubelski *et al.*, 2006), consistent with the notion that LmrR binds the *lmrR* promoter region more strongly than the *lmrCD* promoter region. Consequently, expression of *lmrR* is controlled by a well-tuned and damped feedback autoregulatory loop. This tightly controlled *lmrR* expression may serve to ensure a highly sensitive drug-sensing regulatory mechanism of *lmrCD* expression. High cellular levels of LmrR would render this mechanism less

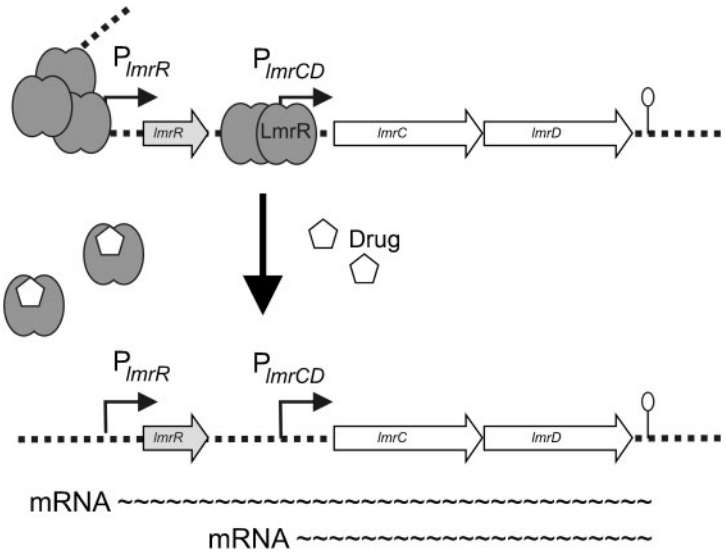

Fig. 7. Schematic representation of the regulation of *lmrR* and *lmrCD* expression by LmrR in *L. lactis*. In wild-type cells growing in drug-free medium, LmrR binds and represses the transcription of both the *lmrCD* gene and the *lmrR* gene. Binding to the *lmrR* operator sequences involves cooperative binding of multiple copies of the LmrR dimer, while LmrR binds as two dimers to the *lmrCD* operator sequences. When cells are challenged with a drug, the LmrR dimer binds a drug molecule and this causes the release of the LmrR–drug complex from the *lmrCD* and *lmrR* operator sequences, allowing the initiation of transcription with the formation of a polycistronic mRNA that supports the translation of both the *lmrR* gene and the *lmrCD* gene, as well as mRNAs harbouring the *lmrCD* genes only.

sensitive to drugs, as increased intracellular drug concentrations would be needed to achieve derepression of *lmrCD* expression. In contrast, direct transcription from the *lmrCD* operator sites is likely more responsive to drugs because of a less extensive LmrR-binding mechanism. Since *lmrR* and *lmrCD* are at least partially co-transcribed, expression of high levels of LmrCD is prevented, as the newly synthesized LmrR will readily repress further transcription. This will for instance minimize the risk that hydrophobic metabolites important to the cell are lost due to uncontrolled and unwanted secretion. Indeed, in the *L. lactis* NZ9000(Δ*lmrR*) strain, higher *lmrCD* transcript levels are observed than in wild-type cells challenged with drugs. Future studies are required to determine the exact stoichiometry of LmrR binding to the various operator sequences and to unravel the molecular details of the LmrR-imposed control of promoter activity (inhibition of closed complex formation, isomerization, promoter clearance).

ACKNOWLEDGEMENTS

We thank Andy-Mark Thunnissen for discussion and valuable suggestions. We thank Structural Biology Brussels (Vrije Universiteit Brussel) for the use of their AFM equipment. E. P. is a postdoctoral fellow of Fonds Wetenschappelijk Onderzoek (FWO)-Vlaanderen.

REFERENCES

Abramoff, M. D., Magelhaes, P. J. & Ram, S. J. (2004). Image processing with ImageJ. *Biophotonics International* **11**, 36–42.

Agustiandari, H., Lubelski, J., van den Berg van Saparoea, H. B., Kuipers, O. P. & Driessen, A. J. M. (2008). LmrR is a transcriptional repressor of expression of the multidrug ABC transporter LmrCD in *Lactococcus lactis*. *J Bacteriol* **190**, 759–763.

Alekshun, M. N. & Levy, S. B. (1997). Regulation of chromosomally mediated multiple antibiotic resistance: the *mar* regulon. *Antimicrob Agents Chemother* **41**, 2067–2075.

Bolhuis, H., Molenaar, D., Poelarends, G., van Veen, H. W., Poolman, B., Driessen, A. J. M. & Konings, W. N. (1994). Proton motive force-driven and ATP-dependent drug extrusion systems in multidrug-resistant *Lactococcus lactis*. *J Bacteriol* **176**, 6957–6964.

Chopra, I. & Roberts, M. (2001). Tetracycline antibiotics: mode of action, applications, molecular biology, and epidemiology of bacterial resistance. *Microbiol Mol Biol Rev* **65**, 232–260.

Eckert, B. & Beck, C. F. (1989). Overproduction of transposon Tn*10*-encoded tetracycline resistance protein results in cell death and loss of membrane potential. *J Bacteriol* **171**, 3557–3559.

Enoru-Eta, J., Gigot, D., Thia-Toong, T. L., Glansdorff, N. & Charlier, D. (2000). Purification and characterization of Sa-lrp, a DNA-binding protein from the extreme thermoacidophilic archaeon *Sulfolobus acidocaldarius* homologous to the bacterial global transcriptional regulator Lrp. *J Bacteriol* **182**, 3661–3672.

Enoru-Eta, J., Gigot, D., Glansdorff, N. & Charlier, D. (2002). High resolution contact probing of the Lrp-like DNA-binding protein Ss-Lrp from the hyperthermoacidophilic crenarchaeote *Sulfolobus solfataricus* P2. *Mol Microbiol* **45**, 1541–1555.

Friedrich, U. & Lenke, J. (2006). Improved enumeration of lactic acid bacteria in mesophilic dairy starter cultures by using multiplex quantitative real-time PCR and flow cytometry-fluorescence in situ hybridization. *Appl Environ Microbiol* **72**, 4163–4171.

Gasson, M. J., Kitamura, Y., McLauchlan, W. R., Narbad, A., Parr, A. J., Parsons, E. L., Payne, J., Rhodes, M. J. & Walton, N. J. (1998). Metabolism of ferulic acid to vanillin. A bacterial gene of the enoyl-SCoA hydratase/isomerase superfamily encodes an enzyme for the hydration and cleavage of a hydroxycinnamic acid SCoA thioester. *J Biol Chem* **273**, 4163–4170.

Grkovic, S., Brown, M. H. & Skurray, R. A. (2002). Regulation of bacterial drug export systems. *Microbiol Mol Biol Rev* **66**, 671–701.

Gury, J., Barthelmebs, L., Tran, N. P., Diviès, C. & Cavin, J. F. (2004). Cloning, deletion, and characterization of PadR, the transcriptional repressor of the phenolic acid decarboxylase-encoding *padA* gene of *Lactobacillus plantarum*. *Appl Environ Microbiol* **70**, 2146–2153.

Hickman, R. K., McMurry, L. M. & Levy, S. B. (1990). Overproduction and purification of the Tn*10*-specified inner membrane tetracycline resistance protein Tet using fusions to β-galactosidase. *Mol Microbiol* **4**, 1241–1251.

Hochschild, A. & Ptashne, M. (1986). Cooperative binding of λ repressors to sites separated by integral turns of the DNA helix. *Cell* **44**, 681–687.

Hsieh, P. C., Siegel, S. A., Rogers, B., Davis, D. & Lewis, K. (1998). Bacteria lacking a multidrug pump: a sensitive tool for drug discovery. *Proc Natl Acad Sci U S A* **95**, 6602–6606.

Huillet, E., Velge, P., Vallaeys, T. & Pardon, P. (2006). LadR, a new PadR-related transcriptional regulator from *Listeria monocytogenes*, negatively regulates the expression of the multidrug efflux pump MdrL. *FEMS Microbiol Lett* **254**, 87–94.

Lubelski, J., Mazurkiewicz, P., van Merkerk, R., Konings, W. N. & Driessen, A. J. M. (2004). *ydaG* and *ydbA* of *Lactococcus lactis* encode a heterodimeric ATP-binding cassette-type multidrug transporter. *J Biol Chem* **279**, 34449–34455.

Lubelski, J., de Jong, A., van Merkerk, R., Agustiandari, H., Kuipers, O. P., Kok, J. & Driessen, A. J. M. (2006). LmrCD is a major multidrug resistance transporter in *Lactococcus lactis*. *Mol Microbiol* **61**, 771–781.

Ma, D., Alberti, M., Lynch, C., Nikaido, H. & Hearst, J. E. (1996). The local repressor AcrR plays a modulating role in the regulation of *acrAB* genes of *Escherichia coli* by global stress signals. *Mol Microbiol* **19**, 101–112.

Madoori, P. K., Agustiandari, H., Driessen, A. J. M. & Thunnissen, A. M. (2009). Structure of the transcriptional regulator LmrR and its mechanism of multidrug recognition. *EMBO J* **28**, 156–166.

Maxam, A. M. & Gilbert, W. (1980). Sequencing end-labeled DNA with base-specific chemical cleavages. *Methods Enzymol* **65**, 499–560.

Mazurkiewicz, P., Driessen, A. J. M. & Konings, W. N. (2004). Energetics of wild-type and mutant multidrug resistance secondary transporter LmrP of *Lactococcus lactis*. *Biochim Biophys Acta* **1658**, 252–261.

Minh, P. N. L., Devroede, N., Massant, J., Maes, D. & Charlier, D. (2009). Insights into the architecture and stoichiometry of *Escherichia coli* PepA*DNA complexes involved in transcriptional control and site-specific DNA recombination by atomic force microscopy. *Nucleic Acids Res* **37**, 1463–1476.

Musso, R. E., Di Lauro, R., Adhya, S. & de Crombrugghe, B. (1977). Dual control for transcription of the galactose operon by cyclic AMP and its receptor protein at two interspersed promoters. *Cell* **12**, 847–854.

Neyfakh, A. A., Bidnenko, V. E. & Chen, L. B. (1991). Efflux-mediated multidrug resistance in *Bacillus subtilis*: similarities and dissimilarities with the mammalian system. *Proc Natl Acad Sci U S A* **88**, 4781–4785.

Neyfakh, A. A., Borsch, C. M. & Kaatz, G. W. (1993). Fluoroquinolone resistance protein NorA of *Staphylococcus aureus* is a multidrug efflux transporter. *Antimicrob Agents Chemother* **37**, 128–129.

Ng, E. Y., Trucksis, M. & Hooper, D. C. (1994). Quinolone resistance mediated by *norA*: physiologic characterization and relationship to *flqB*, a quinolone resistance locus on the *Staphylococcus aureus* chromosome. *Antimicrob Agents Chemother* **38**, 1345–1355.

Overhage, J., Priefert, H. & Steinbüchel, A. (1999). Biochemical and genetic analyses of ferulic acid catabolism in *Pseudomonas* sp. strain HR199. *Appl Environ Microbiol* **65**, 4837–4847.

Paulsen, I. T., Nguyen, L., Sliwinski, M. K., Rabus, R. & Saier, M. H., Jr (2000). Microbial genome analyses: comparative transport capabilities in eighteen prokaryotes. *J Mol Biol* **301**, 75–100.

Peeters, E., Thia-Toong, T. L., Gigot, D., Maes, D. & Charlier, D. (2004). Ss-LrpB, a novel Lrp-like regulator of *Sulfolobus solfataricus* P2, binds cooperatively to three conserved targets in its own control region. *Mol Microbiol* **54**, 321–336.

Peeters, E., Willaert, R., Maes, D. & Charlier, D. (2006). Ss-LrpB from *Sulfolobus solfataricus* condenses about 100 base pairs of its own operator DNA into globular nucleoprotein complexes. *J Biol Chem* **281**, 11721–11728.

Rahmati, S., Yang, S., Davidson, A. L. & Zechiedrich, E. L. (2002). Control of the AcrAB multidrug efflux pump by quorum-sensing regulator SdiA. *Mol Microbiol* **43**, 677–685.

Rivetti, C., Guthold, M. & Bustamante, C. (1996). Scanning force microscopy of DNA deposited onto mica: equilibration versus kinetic trapping studied by statistical polymer chain analysis. *J Mol Biol* **264**, 919–932.

Saier, M. H., Jr, Paulsen, I. T., Sliwinski, M. K., Pao, S. S., Skurray, R. A. & Nikaido, H. (1998). Evolutionary origins of multidrug and drug-specific efflux pumps in bacteria. *FASEB J* **12**, 265–274.

Schumacher, M. A. & Brennan, R. G. (2003). Deciphering the molecular basis of multidrug recognition: crystal structures of the *Staphylococcus aureus* multidrug binding transcription regulator QacR. *Res Microbiol* **154**, 69–77.

Segura, A., Bünz, P. V., D'Argenio, D. A. & Ornston, L. N. (1999). Genetic analysis of a chromosomal region containing *vanA* and *vanB*, genes required for conversion of either ferulate or vanillate to protocatechuate in *Acinetobacter*. *J Bacteriol* **181**, 3494–3504.

Tennent, J. M., Lyon, B. R., Gillespie, M. T., May, J. W. & Skurray, R. A. (1985). Cloning and expression of *Staphylococcus aureus* plasmid-mediated quaternary ammonium resistance in *Escherichia coli*. *Antimicrob Agents Chemother* **27**, 79–83.

Zaidi, A. H., Bakkes, P. J., Lubelski, J., Agustiandari, H., Kuipers, O. P. & Driessen, A. J. M. (2008). The ABC-type multidrug resistance transporter LmrCD is responsible for an extrusion-based mechanism of bile acid resistance in *Lactococcus lactis*. *J Bacteriol* **190**, 7357–7366.

Edited by: A. R. Walmsley

LmrR-mediated gene regulation of multidrug resistance in *Lactococcus lactis*

By: Herfita Agustiandari, Eveline Peeters, Janny G. de Wit, Daniel Charlier and Arnold J. M. Driessen

SUPPLEMENTARY TABLES

Supplementary Table S1. Primer sets used for RT-PCR analysis

Primer	5′→3′ sequence
DC620r	CTCCTTGTTTTAGGACATTGAGC
DC621r	AAGATTGAGAATAAGGCAACCC
DC634f	CGGAGATGATTTTTTCTTATCTTATATAG
DC635f	CTATTGTAATCTTTAACAGCATTAAC
DC636f	ATGGCAGAAATACCAAAAGAATG
CDprmf	GTATTACCGACTGACAGAGATTGG

Supplementary Table S2. Primer sets used for extended EMSA analysis

Primer	5′→3′ sequence
Region 1f	CAAATAAGAAGAGTGAAGCG
Region 1r	GGCAACCCATTTATGCTTCA
Region 2f	ACAAATAACGTCGTAAATCG
Region 2r	GGCAACCCATTTATGCTTCA
Region 3f	ATTGTAATCTTTAACAGCATTAAC
Region 3r	GGCAACCCATTTATGCTTCA
Region 4f	TTCTCAAAAAATTTATTGAAATTA
Region 4r	GGCAACCCATTTATGCTTCA
Region 5f	CAAATAAGAAGAGTGAAGCG
Region 5r	AAATTTTTTGAGAAGATAAT
Region 6f	CAAATAAGAAGAGTGAAGCG
Region 6r	GCATTAACAATTAATGCTTGTTTACT
Region 7f	CAAATAAGAAGAGTGAAGCG
Region 7r	GTTTACCATTTATGAAACTAACTATTG
Region 8f	CAAATAAGAAGAGTGAAGCG
Region 8r	CGTTGACTTAAACTTTAAAAAG

Supplementary Table S3. Primer sets used for qPCR analysis

Primer	5′→3′ sequence	Length	GC content (%)
TufAf	TGACGAAATCGAACGTGGTCAAG	23	47
TufAr	GTCACCAGGCATTACCATTTCAG	23	47
SecYf	GCTTGCTATGGCACAATCTATCG	23	47
SecYr	ATGGCTGATGGAATACCAGAGAC	23	47
LmrRf	ATGTTACGAGCCCAAACCAATG	22	45
LmrRr	TCTGTCAGTCGGTAATACTTGC	22	45
LmrR-Cf	GTATTACCGACTGACAGAGATTG	23	43
LmrR-Cr	GTTTAAGTCAACGATTTACGACG	23	39
LmrCf	GCGAAAGACGAAGAACTTTCTGG	23	47
LmrCr	ACTGAAACAGTCCCTTCTGTTGG	23	47
LmrDf	CGAAAGCTTGCCTGACAAGTATG	23	47
LmrDr	CGAATGAAGTTCGTCCAGCAATG	23	47

LmrR-mediated gene regulation of multidrug resistance in *Lactococcus lactis*

By: Herfita Agustiandari, Eveline Peeters, Janny G. de Wit, Daniel Charlier and Arnold J. M. Driessen

SUPPLEMENTARY FIGURE LEGEND

Supplementary Fig. S1. EMSA of the binding of LmrR to truncated DNA fragments corresponding to different parts of the *lmrCD* control region. The concentration of wild-type LmrR was kept constant (1.85 μM dimer) in all lanes. The −35 and −10 boxes shown belong to the promoter of transcript B. Double-stranded DNA fragments (○) were obtained by PCR using the primers indicated in Supplementary Table S2. The shifted DNA is indicated by ●.

LmrR-mediated gene regulation of multidrug resistance in *Lactococcus lactis*

By: Herfita Agustiandari, Eveline Peeters, Janny G. de Wit, Daniel Charlier and Arnold J. M. Driessen

Supplementary Fig. S1